HuR and GRSF1 modulate the nuclear export and mitochondrial localization of the lncRNA *RMRP*

Ji Heon Noh,[1,4] Kyoung Mi Kim,[1,4] Kotb Abdelmohsen,[1] Je-Hyun Yoon,[1] Amaresh C. Panda,[1] Rachel Munk,[1] Jiyoung Kim,[1] Jessica Curtis,[2] Christopher A. Moad,[3] Christina M. Wohler,[3] Fred E. Indig,[3] Wilson de Paula,[1] Dawood B. Dudekula,[1] Supriyo De,[1] Yulan Piao,[1] Xiaoling Yang,[1] Jennifer L. Martindale,[1] Rafael de Cabo,[2] and Myriam Gorospe[1]

[1]Laboratory of Genetics, [2]Laboratory of Experimental Gerontology, [3]Confocal Imaging Facility, National Institute on Aging, National Institutes of Health, Baltimore, Maryland 21224, USA

Some mitochondrial long noncoding RNAs (lncRNAs) are encoded by nuclear DNA, but the mechanisms that mediate their transport to mitochondria are poorly characterized. Using affinity RNA pull-down followed by mass spectrometry analysis, we found two RNA-binding proteins (RBPs), HuR (human antigen R) and GRSF1 (G-rich RNA sequence-binding factor 1), that associated with the nuclear DNA-encoded lncRNA *RMRP* and mobilized it to mitochondria. In cultured human cells, HuR bound *RMRP* in the nucleus and mediated its CRM1 (chromosome region maintenance 1)-dependent export to the cytosol. After *RMRP* was imported into mitochondria, GRSF1 bound *RMRP* and increased its abundance in the matrix. Loss of GRSF1 lowered the mitochondrial levels of *RMRP*, in turn suppressing oxygen consumption rates and modestly reducing mitochondrial DNA replication priming. Our findings indicate that RBPs HuR and GRSF1 govern the cytoplasmic and mitochondrial localization of the lncRNA *RMRP*, which is encoded by nuclear DNA but has key functions in mitochondria.

[*Keywords*: RNA-binding proteins; nuclear RNA export; ribonucleoprotein complex; mitochondrial RNA import; oxygen consumption rate]

Supplemental material is available for this article.

Received December 6, 2015; revised version accepted April 14, 2016.

Human mitochondrial DNA (mtDNA) contains 13 genes encoding protein components of the mitochondrial oxidative phosphorylation (OXPHOS) system, 22 tRNAs, and two rRNAs (*12S* and *16S*) (Anderson et al. 1981). However, a large proportion of mitochondrial proteins necessary for maintaining mitochondrial structure and function are encoded by the nuclear genome, synthesized in the cytoplasm, and imported into mitochondria. In addition, several noncoding RNAs (ncRNAs) transcribed in the nucleus but residing in mitochondria also play a key role in regulating mitochondrial gene expression (Chang and Clayton 1987; Smirnov et al. 2011). The molecular mechanisms regulating the process of RNA import into the mitochondria are only now beginning to emerge. One study identified a cytosolic protein, rhodanese, as an import factor directing cytoplasmic *5S* rRNA (encoded by nuclear DNA) into the mitochondrial matrix (Smirnov et al. 2010). Another study implicated the RNA import factor polynucleotide phosphorylase (PNPase), located in the mitochondrial intermembrane space (IMS), as a mediator of the translocation of cytosolic RNAs into mitochondria, possibly requiring additional proteins to translocate RNA through the inner membrane (IM) into the matrix (Wang et al. 2010). Together, these results suggest that a series of proteins or protein complexes mediates RNA transport from the nucleus to mitochondria.

Analysis of the mitochondrial transcriptome (our RNA sequencing [RNA-seq] data [GSE73458]; Mercer et al. 2011) led to the systematic identification of several nuclear DNA-encoded long ncRNAs (lncRNAs) present in the mitochondrial inner compartment, the matrix. Among these, *RMRP* (the RNA component of the RNA processing endoribonuclease [RNase MRP]) was found to associate with the RNA-binding proteins (RBPs) HuR (human antigen R) and GRSF1 (G-rich RNA sequence-binding

[4]**These authors contributed equally to this work.**
Corresponding author: myriam-gorospe@nih.gov
Article published online ahead of print. Article and publication date are online at http://www.genesdev.org/cgi/doi/10.1101/gad.276022.115.

factor 1). *RMRP* is best known for being a component of the nuclear RNase MRP complex, which participates in the processing of ribosomal RNA to generate the short mature *5.8S* rRNA (Schmitt and Clayton 1993) and cleaves B-cyclin (*CLB2*) mRNA in yeast, lowering B-cyclin levels during mitosis (Gill et al. 2004). In addition, *RMRP* interacts with telomerase to form a complex with RNA-dependent RNA polymerase activity capable of synthesizing dsRNA precursors processed by DICER1 into siRNAs (Maida et al. 2009). As a component of the mitochondrial RNase MRP, *RMRP* is important for mitochondrial DNA replication and RNA processing (Chang and Clayton 1987, 1989). Given the essential mitochondrial functions of *RMRP*, identifying RBPs involved in transporting and modulating *RMRP* actions in mitochondria is critical. We thus set out to investigate the interactions of *RMRP* with HuR and GRSF1 in depth.

A member of the ELAV (embryonic lethal abnormal vision) family of RBPs, HuR is a ubiquitous protein that interacts with target RNAs via its three RNA recognition motifs (RRMs). HuR has been implicated in numerous post-transcriptional gene regulatory events, including nuclear mRNA export, mRNA stabilization, and translation (Fan and Steitz 1998; Abdelmohsen and Gorospe 2010). Although HuR is predominantly nuclear, it can shuttle across the nuclear envelope, in some cases mobilizing target mRNAs in the process (Gallouzi and Steitz 2001; Prechtel et al. 2006; Doller et al. 2008; Yi et al. 2010). Transcriptome-wide analyses of HuR target RNAs using photoactivatable ribonucleoside-enhanced cross-linking and immunoprecipitation (PAR-CLIP) revealed numerous coding RNA and ncRNA ligands for HuR and indicated that HuR influenced the stability of mature mRNAs and possibly other aspects of their post-transcriptional fate (Kishore et al. 2011; Lebedeva et al. 2011; Mukherjee et al. 2011). Although HuR can also bind ncRNAs (e.g., lncRNAs and microRNAs), the impact of HuR on ncRNAs has been reported for only a few targets (Yoon et al. 2012, 2013). The RBP GRSF1 is also a ubiquitous RBP and bears three RRMs. It was first identified as a cytoplasmic RBP with high affinity for G-rich sequences (Qian and Wilusz 1994) and was shown to regulate viral and cellular RNA metabolism at many levels, including splicing, polyadenylation, export, and recruitment to polysomes (Ufer 2012). Recent reports have implicated GRSF1 in mitochondrial-related processes, as it was found in submitochondrial domains termed "RNA granules" and was found to interact physically with mtDNA-encoded transcripts (mtRNAs), regulate mitochondrial gene expression post-transcriptionally, and help assemble the mitochondrial ribosome (Antonicka et al. 2013; Jourdain et al. 2013).

Our results presented here indicate that *RMRP*, transcribed from nuclear DNA, can be mobilized into the cytosol and accumulate in the mitochondrial matrix by the RBPs HuR and GRSF1, respectively. These findings suggest novel roles for RBPs in the transport and localization of ncRNAs to mitochondria and provide new knowledge of the mechanisms through which regulatory RNAs are mobilized across cellular organelles.

Results

Transcribed in the nucleus, mitochondria-resident lncRNA RMRP *binds to the RBPs HuR and GRSF1*

In order to investigate the mechanisms that govern the mitochondrial import of RNAs transcribed in the nucleus, RNA-seq was performed to analyze the transcriptome profile in the mitoplast, the compartment within the mitochondrial IM (Materials and Methods) of WI-38 human fibroblasts (GSE73458). We identified numerous ncRNAs encoded by nuclear DNA, including many ncRNAs that overlapped with those identified by Mercer et al. (2011) (Supplemental Fig. S1A). Among the nuclear DNA-encoded ncRNAs found in mitochondria from our RNA-seq analysis (Supplemental Fig. S1B), we focused on *RMRP*, the RNA component of the RNase MRP ribonucleoprotein (RNP) complex, which plays a key role in mitochondrial metabolism and gene regulation (Chang and Clayton 1987).

To comprehensively identify all of the cellular RBPs that interact with *RMRP*, we performed RNA pull-down assays followed by mass spectrometry (MS). Biotinylated antisense (AS; binding to *RMRP*) or sense (S; nonbinding negative control) oligomers (Supplemental Fig. S2A) were incubated with whole-cell extracts of human embryonic kidney 293 (HEK293) cells (Fig. 1A). Streptavidin-coated agarose beads were used to pull down RNP complexes, and the bound proteins were separated by SDS-PAGE and visualized by staining using Coomassie blue dye. As anticipated, *RMRP* was enriched in the pull-down material (Fig. 1B, left), and several protein bands were readily detected in samples pulled down with AS oligomers that were either absent or only weakly present in S oligomer pull-down samples (Fig. 1B, right). The most prominent bands in the AS pull-down material were excised and analyzed by MS. Additional proteins enriched in the AS pull-down were known *RMRP*-interacting proteins such as RPP38 and hPOP1 (Lygerou et al. 1996; Pluk et al. 1999; data not shown). Among the proteins present in the most prominent bands, we identified two well-known RBPs: ELAVL1/HuR (~40 kDa) and GRSF1 (50–60 kDa) (Fig. 1B, right). HuR was chosen for further analysis, as earlier cross-linking experiments showed that it interacts with *RMRP* (Kishore et al. 2011), while similar evidence did not exist for other RBPs from the MS data set (Supplemental Fig. S2B). GRSF1 was investigated further because it was one of the prominent mitochondrial RBPs found among the proteins identified by MS (Supplemental Fig. S2C). Other RBPs identified by MS (Supplemental Fig. S2B, cutoff >15 peptides) were also tested, including HNRNPH, HNRNPF, and HNRNPC; these RBPs showed only modest interaction with *RMRP* and did not influence its subcellular distribution (data not shown). By Western blot analysis, we confirmed that HuR and GRSF1 were enriched in the AS pull-down material (Fig. 1C).

To verify these interactions using other methods, we carried out RNP immunoprecipitation (RIP) analysis. After immunoprecipitation using anti-HuR or control IgG antibodies (Fig. 1D), RNA was extracted from the

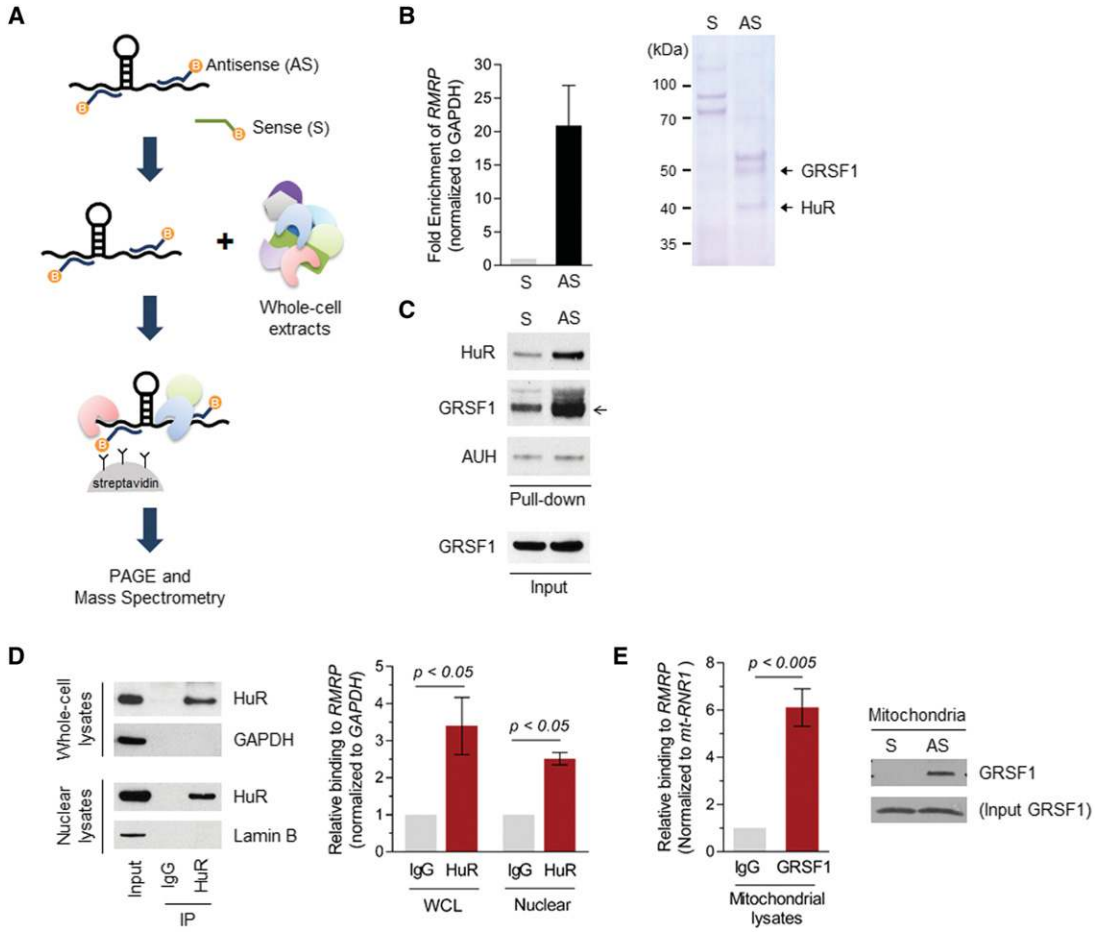

Figure 1. HuR and GRSF1 bind *RMRP*. (*A*) Schematic representation of RNA pull-down experiments to identify *RMRP*-associated proteins. Biotinylated oligomers targeting *RMRP* (AS) or serving as a control (S) were incubated with HEK293 whole-cell extracts and pulled down using streptavidin beads. The pull-down material was washed, and the associated proteins were resolved by gel electrophoresis; specific bands were cut and identified by MS. (*B*, *left*) The relative enrichment of *RMRP* in the pull-down material was measured by RT-qPCR analysis. (*Right*) The two prominent bands in the *AS* pull-down (at ~40 and 50 kDa) contained the RBPs HuR and GRSF1, respectively. (*C*) Western blot analysis revealed a specific association of HuR and GRSF1 with endogenous, affinity pulled down *RMRP*. AUH levels were included as a negative, background control. (*D*) HuR RIP analysis in whole-cell or nuclear lysates of HeLa cells. Following immunoprecipitation using anti-HuR antibody or IgG, the presence of HuR in the immunoprecipitated material was assayed by Western blot analysis (*left*), and the enrichment of *RMRP* in HuR immunoprecipitation was assessed by RT-qPCR analysis using specific primers (*right*). GAPDH or Lamin B was detected as a negative control (*left*), and sample input differences were normalized using *GAPDH* mRNA detected in RNA from the same immunoprecipitation samples (*right*). (*E*, *left*) *RMRP* levels were measured by RT-qPCR following RIP analysis to monitor the enrichment of *RMRP* in GRSF1 immunoprecipitation relative to control immunoprecipitation samples present in mitochondrial lysates (Materials and Methods) after normalization to *mt-RNR1* levels. (*Right*) The levels of GRSF1 associated with endogenous *RMRP*—pulled down from mitochondria lysates using AS oligomers as described above—were assessed by Western blot analysis. Data in *B*, *D*, and *E* are the means and SD from three or more independent experiments.

immunoprecipitated material and subjected to RT-qPCR analysis using *RMRP*-specific primers. As shown, endogenous HuR associated selectively with endogenous *RMRP*, as evidenced by the enrichment in *RMRP* levels in HuR immunoprecipitation relative to control IgG immunoprecipitation samples from whole-cell and nuclear lysates prepared from cervical carcinoma HeLa cells (Fig. 1D). A known HuR target (*VHL* mRNA, a positive control) was also enriched in these samples (Supplemental Fig. S2D); *GAPDH* mRNA was used as a normalization control. RIP analysis using IgG and anti-GRSF1 antibodies and mitochondria lysates (Materials and Methods) revealed that *RMRP* in mitochondria was strongly enriched in GRSF1 RIP samples (Fig. 1E, left). Also, endogenous *RMRP* captured by AS oligomers from mitochondria lysate was shown to interact with GRSF1 (Fig. 1E, right). Together, these findings indicate that *RMRP* can associate with two RBPs, HuR and GRSF1, present in the nucleus and mitochondria, respectively.

HuR facilitates the nuclear export of RMRP

A fraction of *RMRP* is mobilized to the mitochondria to function in mtDNA replication and RNA processing

(Chang and Clayton 1987, 1989), but the mechanism by which this nuclear DNA-encoded RNA is transported to the mitochondria is unknown. Since the RBP HuR can export nuclear mRNAs (Brennan et al. 2000) and binds *RMRP* (Fig. 1), we postulated that HuR might help export *RMRP* out of the nucleus and thus increase the cytoplasmic pool of *RMRP*. To test this hypothesis, HuR was silenced in HEK293 embryonic kidney cells by siRNA transfection. HuR levels were strongly reduced in HuR siRNA relative to control populations, as determined by Western blot analysis (Fig. 2A, left), in both the nuclear fraction, where most of HuR resides, and the cytoplasmic fraction; Lamin B and HSP90 served as specific nuclear and cytoplasmic markers, respectively (Fig. 2B). While the steady-state level of *RMRP* was not affected by HuR silencing (Fig. 2A, right), we sought to test whether reducing HuR levels affected the export of *RMRP*. We investigated this possibility by assessing de novo synthesized *RMRP*, which reduced concerns of possible contamination from pre-existing *RMRP* and allowed the specific analysis of newly transcribed *RMRP*. After a brief incubation of HEK293 cells with 4-thiouridine (4SU), which was

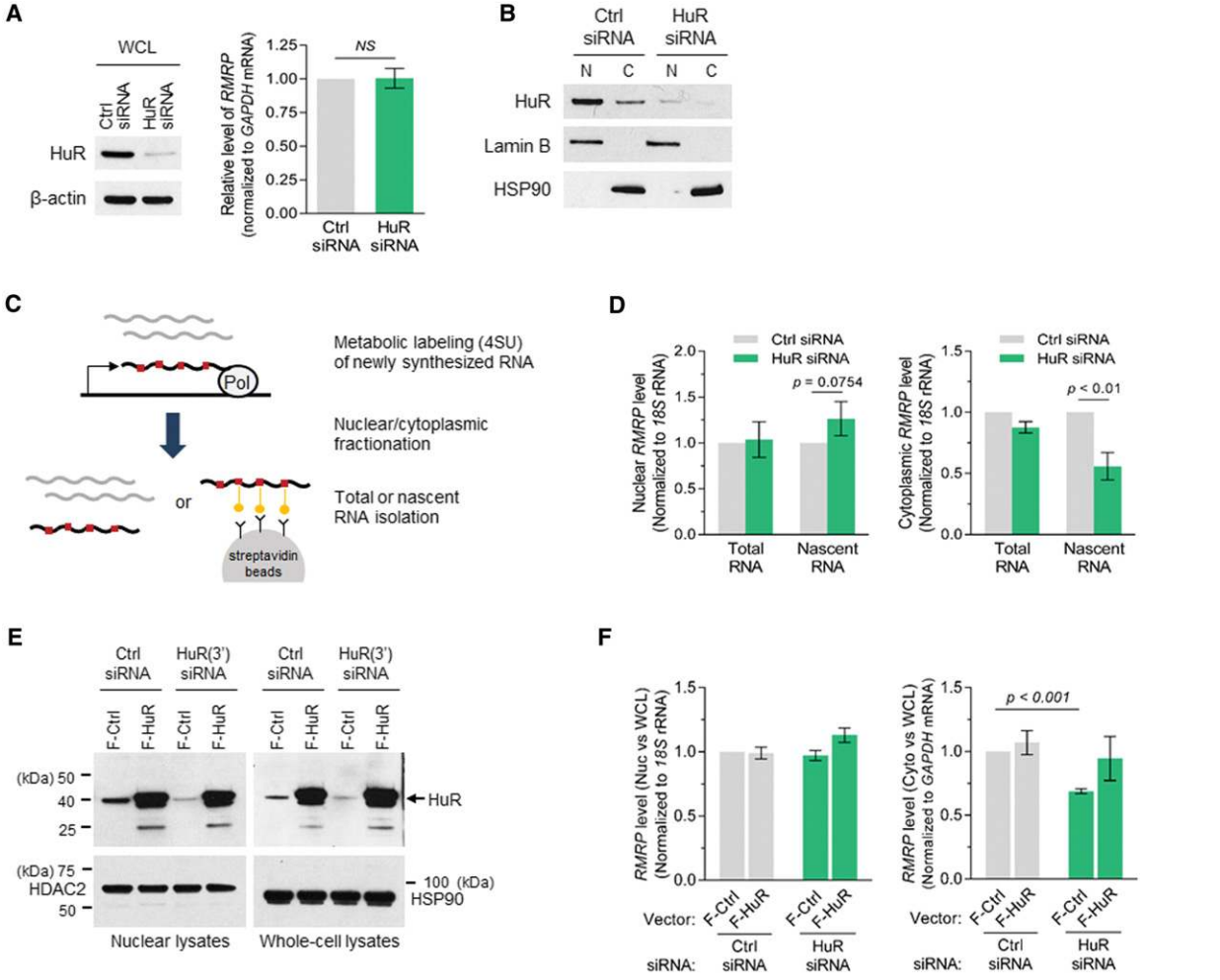

Figure 2. HuR facilitates the export of *RMRP* from the nucleus to the cytoplasm. (*A*,*B*) Forty-eight hours after transfection of either control (Ctrl) or HuR-directed (HuR) siRNAs, whole-cell lysates (WCLs) (*A*) or nuclear (N) and cytoplasmic (C) fractions (*B*) were prepared from HEK293 cells, and the levels of HuR in each compartment were monitored by Western blot analysis; β-actin (*A*, *left*) was used as a loading control, and nuclear protein Lamin B and cytoplasmic protein HSP90 were included as markers to monitor the quality of the fractionation (*B*). (*A*, *right*) *RMRP* levels in total RNA were measured in HuR silenced HEK293 cells. (*C*) Schematic representation of the metabolic RNA labeling with 4SU and the total or nascent RNA isolation from nuclear/cytoplasmic cellular fractions. (*D*) Sixty hours after transfecting HuR siRNA, cells were incubated with 4SU for 12 h, and the nascent 4SU-labeled RNA was tagged with biotin; after fractionation of cells into cytoplasmic and nuclear components, the levels of *RMRP* were measured by RT-qPCR analysis in "total RNA" (including nascent and pre-existing RNA) as well as in biotinylated, "nascent RNA" pulled down using streptavidin beads. (*E*,*F*) Twenty-four hours after transfecting HEK293 cells with *HuR* siRNA (directed at the 3′ UTR of the HuR mRNA) or control siRNA, Flag-tagged HuR (or control vector [F-Ctrl]) was cotransfected, and cells were cultured for an additional 48 h. (*E*) Western blot analysis of HuR, nuclear marker HDAC2, and loading control HSP90 in the fractions is shown. (*F*) As above, during the final 12 h, 4SU was added to the culture medium to label RNA, and then nascent RNA was biotinylated and isolated from nuclear (Nuc), cytoplasmic (Cyto), or whole-cell (WCL) preparations for RT-qPCR analysis. Data in *A*, *D*, and *F* are the means and SD from three or more independent experiments.

incorporated into nascent RNA, 4SU-labeled RNA was tagged with biotin and affinity-purified using streptavidin beads (Fig. 2C). *RMRP* levels were then measured by RT-qPCR in "total RNA" (including labeled and unlabeled RNA) and "nascent RNA" (4SU/biotinylated RNA) extracted from nuclear and cytoplasmic lysates (Fig. 2D). To monitor the quality of RNA following fractionation, a nuclear lncRNA (*NEAT1*) was measured in the nuclear and cytoplasmic preparations (Supplemental Fig. S3A). Our results indicate that silencing HuR only modestly increased *RMRP* levels in the nucleus (Fig. 2D, left), but the export of nuclear (nascent) *RMRP* to the cytoplasm was strongly reduced (by 45%) (Fig. 2D, right), supporting the notion that HuR contributed actively to the cytoplasmic export of *RMRP*. Rescue experiments in which HuR was reintroduced confirmed this result. As shown, silencing HuR using siRNA directed at the *HuR* mRNA 3′ untranslated region (UTR) (Fig. 2E) reduced nascent *RMRP* export to the cytoplasm, but this reduction was rescued by overexpressing a Flag-tagged HuR that lacked a 3′ UTR and was thus refractory to the silencing intervention (Fig. 2F).

MS analysis revealed that *RMRP* associates with several nucleoporins, among which two proteins, PHAX and RanGTPase (data not shown), are important for exporting U snRNAs in a manner dependent on CRM1 (chromosome region maintenance 1), a member of the importin β superfamily of nuclear transport receptors (Ohno et al. 2000). Since CRM1 is a well-known export factor for HuR (Brennan et al. 2000), we sought to suppress CRM1 in order to test whether preventing the nuclear export of HuR would affect *RMRP* levels in the cytoplasm. Silencing CRM1 blocked HuR export, increasing its nuclear levels and reducing its cytoplasmic levels (Fig. 3A). When CRM1 was silenced, cytoplasmic *RMRP* levels declined significantly, while *RMRP* steady-state levels were unchanged (Fig. 3B). Importantly, there was no additional decrease in cytoplasmic *RMRP* when both CRM1 and HuR were silenced jointly (Fig. 3B), and HuR binding to *RMRP* was not affected by CRM1 silencing (Fig. 3C). These observations support the view that the accumulation of *RMRP* in the nucleus was linked to the blocked export of HuR to the cytosol.

HuR PAR-CLIP analysis (Kishore et al. 2011) indicated that HuR interacts with both the 5′ and 3′ segments of *RMRP* (Supplemental Fig. S3C). A number of in vitro transcribed, biotinylated RNAs spanning the length of *RMRP* were synthesized (Fig. 3D; Supplemental Fig. S3D), purified, incubated with HEK293 cell lysates, and pulled down using streptavidin beads to detect bound proteins by Western blot analysis. As shown in Figure 3E, HuR interacted most strongly with the full-length segment as well as with partial fragments f1 and f5, both of which contained the predicted 5′ end HuR-binding site; HuR showed reduced interaction with other fragments but was absent from the negative control lane ("beads"), and the negative control protein (GAPDH) did not bind to the RNAs. Since HuR promoted *RMRP* export to the cytoplasm (Fig. 2), we asked whether it might also direct cytoplasmic *RMRP* to the mitochondria and increase mitochondrial *RMRP* levels. We first assessed whether HuR might be present inside mitochondria. For this, we purified mitochondria and eliminated any contaminating nuclear RNA and protein by incubating the mitochondrial preparation with RNase A and proteinase K (PK), which readily enter nuclei through nucleopores but do not penetrate mitochondria. After hypotonic shock to lyse the outer membrane (OM), we further incubated the contents protected by the IM (the mitoplast) with RNase A and PK. As shown, HuR was not present in the purified mitoplast (Fig. 3F), and HuR silencing did not robustly change the levels of *RMRP* in mitochondria (Fig. 3G), suggesting that simply elevating *RMRP* in the cytoplasm was not sufficient to increase the levels of *RMRP* in the mitochondria, likely because other factors may be involved in actively promoting the mitochondrial localization of *RMRP*. In summary, HuR was found to promote the export of *RMRP* to the cytoplasm in a CRM1-dependent manner (Fig. 3H).

GRSF1 increases RMRP *abundance in mitochondria*

As described above, GRSF1 was also identified as a protein capable of interacting with *RMRP* (Fig. 1). To begin to study the consequences of GRSF1 binding to *RMRP*, we first investigated the precise localization of GRSF1 within mitochondria. Western blot analysis confirmed the presence of GRSF1 inside the matrix, prepared by sequential incubation with RNase A and PK before and after osmotic shock to break the OM in order to eliminate all contaminating RNA and protein from outside the matrix (Materials and Methods). A control mitochondrial matrix-resident protein, Aconitase 2 (ACO2), was protected from digestion (Supplemental Fig. S4A, left). Matrix-resident RNAs (*mt-RNR1*, *mt-ATP6*, *mt-CO1*, and *mt-CYB*) were abundant, as detected by RT-qPCR analysis (Supplemental Fig. S4A, right), while transcripts residing in the nucleus (e.g., lncRNAs *NEAT1* and *MALAT1*) were extremely low. To determine whether there was residual nuclear contamination, the fusion protein MS2-YFP, which bears a strong nuclear localization signal, was expressed in HEK293 cells. In mitoplast fractions, the mitochondrial matrix protein Twinkle was abundant, but MS2-YFP was not (Supplemental Fig. S4B), indicating that the mitochondrial preparation was not contaminated with nuclear components.

HEK293 cells stably overexpressing Flag-tagged full-length GRSF1 with an N-terminal mitochondrial targeting signal (MTS) (Jourdain et al. 2013) showed relatively high *RMRP* levels in whole-cell lysates and even higher levels in the mitochondria, as compared with parental HEK293 cells (Fig. 4A). Conversely, GRSF1 silencing did not affect *RMRP* levels in whole-cell lysates but robustly reduced *RMRP* levels in purified mitochondria, as assessed by RT-qPCR analysis (Fig. 4B). This effect appeared specific, as *mt-RNR1* levels were not affected by GRSF1 silencing, while *mtATP6* and *mt-CYB* were lower when GRSF1 was silenced, as reported (Supplemental Fig. S4C; Antonicka et al. 2013). We then measured endogenous *RMRP* levels in mitoplasts isolated from HEK293 cells after silencing GRSF1 or IMMT (also known as

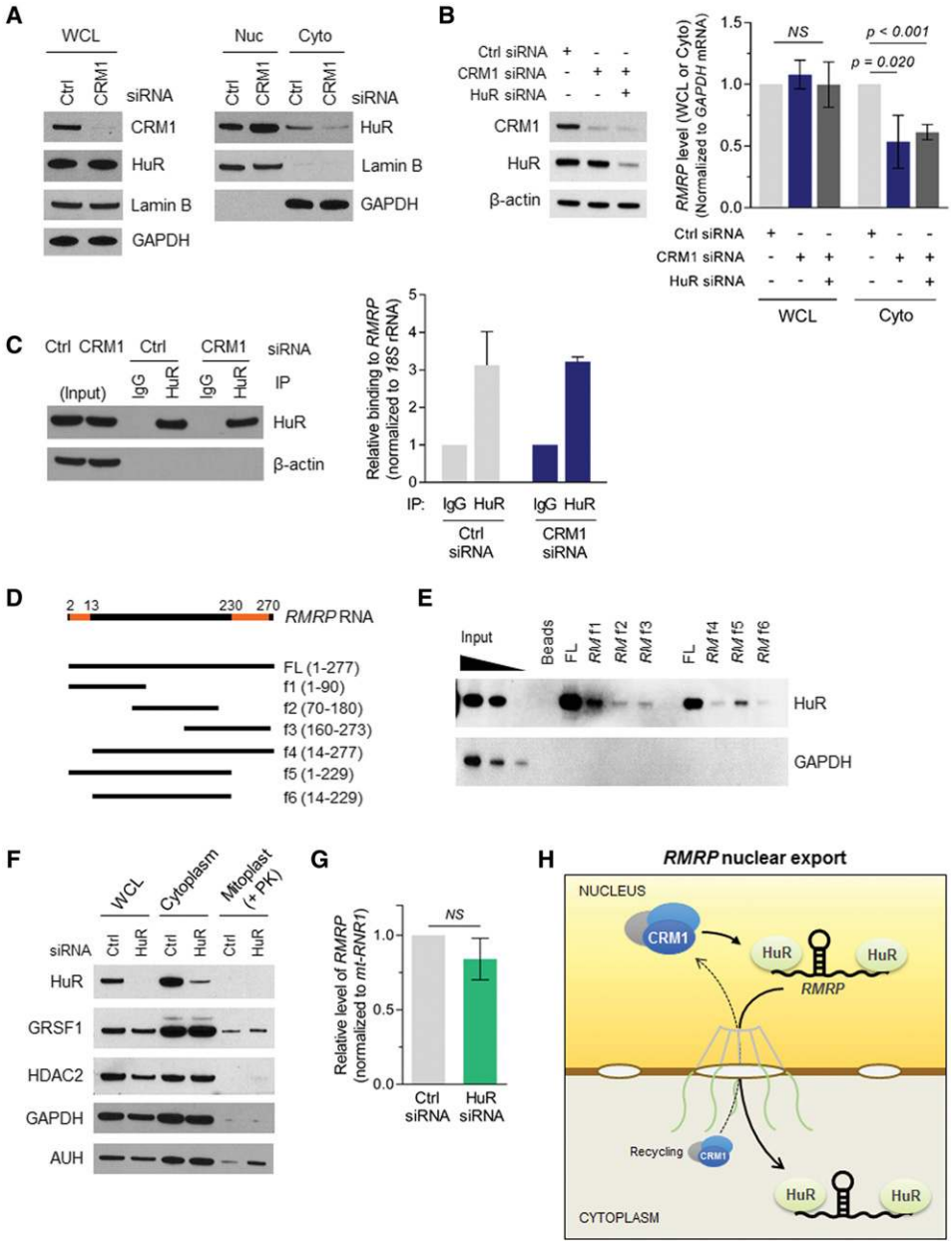

Figure 3. HuR modulates CRM1-dependent export of *RMRP*. (*A*) Seventy-two hours after transfection of control (Ctrl) or CRM1 siRNAs, whole-cell lysates (WCL) and nuclear (Nuc) and cytoplasmic (Cyto) lysates were prepared, and the levels of CRM1 or HuR were detected by Western blot analysis. Lamin B and GAPDH served as loading controls and markers of fractionation. (*B*) After silencing CRM1 and HuR as in *A*, the levels of CRM1 and HuR (and loading control β-actin) were assessed by Western blot analysis. (*Right*) In RNA isolated from whole cells or cytoplasmic fractions, *RMRP* levels were measured by RT-qPCR and normalized to *GAPDH* mRNA levels. (*C*) Forty-eight hours after CRM1 silencing, HuR RIP was performed, HuR levels were assayed by Western blot analysis (*left*), and the enrichment of *RMRP* in HuR immunoprecipitation was assayed by RT-qPCR analysis (*right*). β-Actin was detected as a negative control (*left*), and sample input differences were normalized using *18S* rRNA (*right*). (*D*) Schematic depiction of *RMRP* and the biotinylated fragments synthesized in vitro. (*Top*) Two predicted HuR-binding sites are highlighted. (FL) Full-length *RMRP*; (f1 to f6) *RMRP* deletion fragments. (*E*) HuR interaction with the different segments of *RMRP* was assessed by Western blot analysis in each of the biotin pull-down reactions. "Input" indicates 16, 8, and 4 µg of lysates, and "beads" indicates pull-down reactions without biotinylated RNA. (*F*) Forty-eight hours after transfecting HuR or control siRNAs, HEK293 cells were either left intact (WCL) or fractionated into "cytoplasmic" or "mitoplast" (treated with proteinase K [+PK] fractions) (Materials and Methods); the levels of HuR and GRSF1 were assessed by Western blot analysis. Nuclear (HDAC2), cytoplasmic (GAPDH), and mitochondrial (AUH) proteins served to monitor the quality of the fractionation. (*G*) Mitochondria was further digested with RNase A to eliminate all nuclear and cytosolic RNA contamination; the levels of *RMRP* were measured by RT-qPCR and normalized to the levels of *mt-RNR1*. (*H*) Proposed model of HuR-mediated export of *RMRP* from the nucleus into the cytoplasm. Data in *B*, *C*, and *G* are the means and SD from three or more independent experiments. Data in *A*–*C*, *E*, and *F* are representative of three independent experiments.

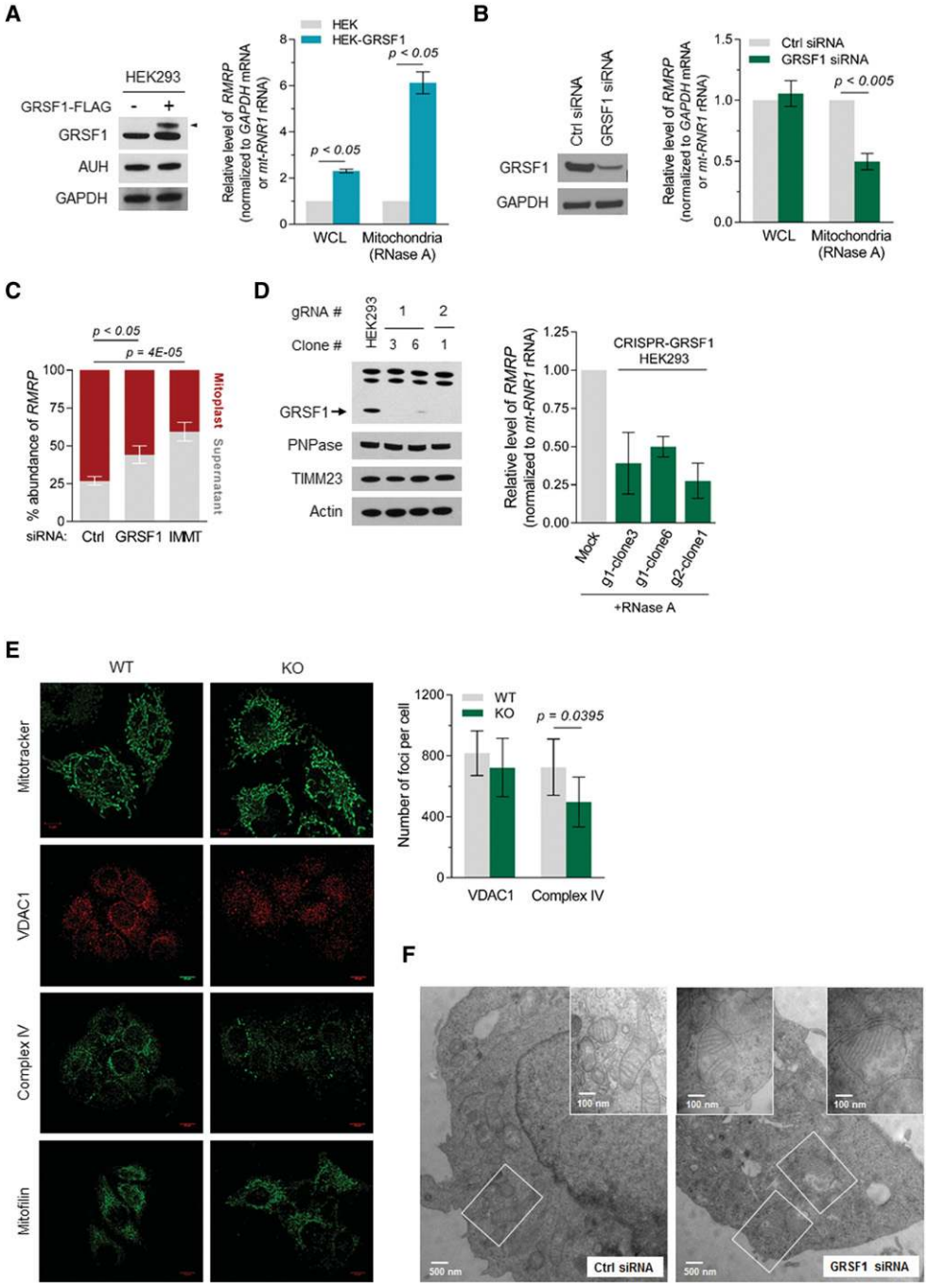

Figure 4. GRSF1 increases *RMRP* abundance in mitochondria. (*A*, *left*) In HEK293 cells stably expressing GRSF1, the levels of GRSF1, GRSF1-Flag (arrowhead), AUH, and GAPDH were assessed by Western blot analysis. (*Right*) *RMRP* levels in total RNA and mitochondrial RNA (after RNase A treatment to eliminate all external RNA, +RNase A) were measured by RT-qPCR analysis. (*B*) Seventy-two hours after transfection of control (Ctrl) or GRSF1 siRNAs, GRSF1 abundance was assessed by Western blot analysis, and *RMRP* levels in whole cells and mitochondria (+RNase A) were measured by RT-qPCR analysis. (*C*) Forty-eight hours after silencing GRSF1 or IMMT in HEK293 cells, mitochondria were isolated and fractionated into mitoplast and the supernatant (Materials and Methods), and *RMRP* levels were assessed by RT-qPCR analysis. (*D*) GRSF1 knockout clonal lines were established in HEK293 cells using CRISPR–Cas9; three clones from two GRSF1-specific guide RNAs were studied further. In the three clones and parental cells, the levels of GRSF1, PNPase, TIMM23, and Actin were assessed by Western blot analysis (*left*), and the levels of *RMRP* in mitochondria were assessed by RT-qPCR analysis (*right*). (*E*) HEK293 cells were grown on MatTek dishes and stained with Mitotracker or incubated with antibodies recognizing VDAC1, complex IV, or mitofilin (Supplemental Material). *Z*-sections were obtained with iSIM, deconvolved with the iSIM software, and analyzed with ImageJ software. (*F*) Mitochondrial morphology as observed by using transmission electron microscopy (TEM) in GRSF1-depleted HEK293 cells. Enlarged fields are shown. Bars, 500 and 100 nm. Data in *A*–*E* are the means and SD from three independent experiments. Data in *A*, *B*, and *D*–*F* are representative of three or more experiments.

mitofilin); after osmotic shock and centrifugation, the supernatants were collected, and the mitoplast pellets were treated with RNase A/PK as described above (Supplemental Fig. S4D,E). As shown in Figure 4C, *RMRP* levels were significantly lower in mitoplasts from GRSF1 silenced cells and IMMT silenced cells than from control cells; mtDNA-encoded RNAs *mt-CYB* and *mt-RNR1* were detected robustly in the mitoplast preparations, indicating that the supernatant has negligible amounts of RNA leaked from mitoplasts (Supplemental Fig. S4F). These observations further support the idea that GRSF1 elevates *RMRP* levels in mitochondria.

Further support for the idea that GRSF1 contributed to elevating mitochondrial *RMRP* levels came from studies in which GRSF1 was knocked out in HEK293 cells using the CRISPR–Cas9 system (Materials and Methods; Fig. 4D, left). Importantly, knocking out GRSF1 caused a marked decline in the levels of *RMRP* in mitochondria, as assessed by RT-qPCR analysis (Fig. 4D, right), further supporting a role for GRSF1 in enhancing *RMRP* presence in mitochondria.

To test whether impairment of GRSF1 and *RMRP* levels affected mitochondrial morphology and distribution, we stained mitochondria from wild-type and GRSF1 knockout HEK293 cells using MitoTracker and detected mitochondrial structural proteins (VDAC1, complex IV, and mitofilin) by immunofluorescence. We did not observe striking changes in the density or morphology of mitochondria when comparing wild-type and GRSF1 knockout cells (Fig. 4E). However, the signal for an enzyme of the electron transport chain, complex IV (cytochrome c oxidase), was significantly lower in GRSF1 knockout cells (Fig. 4E, graph). We further investigated whether GRSF1 affected membrane and cristae structure by assessing wild-type and GRSF1-depleted mitochondria using transmission electron microscopy (TEM). As shown in Figure 4F, unlike the highly ordered cristae observed in mitochondria from control cells, the mitochondria in GRSF1 silenced cells showed the defects in IM cristae shape (Fig. 4F). Collectively, these results suggest that mitochondrial GRSF1 enhances the accumulation of *RMRP* in mitochondria, an effect that was linked to the control of IM organization and GRSF1 function contributing to the maintenance of the OXPHOS complex.

RMRP internalization and accumulation in mitochondria

GRSF1 was previously found to interact with the G-rich sequence $A(G)_4A$ present in the 5′ UTR of *m-GPx4* mRNA, which encodes the mitochondrial isoform of phospholipid hydroperoxide glutathione peroxidase (Ufer et al. 2008). We found the same $A(G)_4A$ motif in the *RMRP* sequence as well as a predicted stem sequence (an internal stem) (Supplemental Fig. S2A). To test more directly the possibility that GRSF1 promotes the localization of *RMRP* in mitochondria, we measured the import of exogenous *RMRP* (bearing a sequence tag for specific PCR amplification) (Fig. 5A) that was either full-length (*RMRP_FL*) or truncated at the 5′ end and hence lacking the G-rich sequence and the first, conserved, stem–loop structure (*RMRP_f2/f3*). Plasmid vectors expressing tagged *RMRP_FL* and *RMRP_f2/f3* RNAs were created and transfected into HEK293 cells; after selection and clonal expansion, mitochondria were isolated from each cell population for in vivo import analysis. As measured by using specific PCR primers that selectively recognize the PCR tag, both *RMRP* transcripts were expressed at comparable levels ($RNase^-$ samples), while only *RMRP_FL* was effectively protected from degradation ($RNase^+$ samples), indicating that the *RMRP_FL* transcript was preferentially internalized into mitochondria (Fig. 5B).

In vitro mitochondrial import assays were then performed using in vitro transcribed, radiolabeled *RMRP_FL* and *RMRP_f2/f3* and control transcript *GAPDH* 3′ UTR. The recombinant transcripts used are shown (Fig. 5C, "input RNA"). The radiolabeled *GAPDH* 3′ UTR and *RMRP_FL*, and *RMRP_f2/f3* RNAs were incubated with isolated mitochondria, and the import into mitochondria was assessed by measuring radioactive RNA inside mitochondria 15 min later. As shown in Figure 5C, the *GAPDH* 3′ UTR and *RMRP_f2/f3* were modestly internalized (17% and 6% of input, respectively), while internalization of *RMRP_FL* was significantly more robust (74% of the total); as expected, most of the internalized *RMRP_FL* was cleaved into an ~130-nucleotide (nt)-long segment (Chang and Clayton 1987; Wang et al. 2010). Given that both the G-rich sequence and the stem structure (Supplemental Fig. S2A) were absent from *RMRP_f2/f3*, we generated additional mutant *RMRP*s, as shown (Fig. 5D, top), and studied their import into mouse liver mitochondria. Radiolabeled *RMRP* wild type, *RMRP* lacking the G-rich element [GGGG (67–70 nt) → TTTT, mut1], *RMRP* unable to form a stem [CCCG (77–80 nt) → AAAT, mut2], and *RMRP* bearing both mutations (mut1+2) were incubated with mouse liver mitochondria, and, 15 min later, the amount of radiolabeled RNA in the mitochondria was assessed. As shown (Fig. 5D), compared with *RMRP* wild type, the G-rich mutant (mut1) showed slightly lower *RMRP* import, the stem–loop mutant (mut2) showed import comparable with that of *RMRP* wild type, and the double mutant (mut1+2) showed a robust reduction in signal. Input RNA and protein (AUH) are shown (Fig. 5D, bottom). Finally, the import of radiolabeled *RMRP* wild type into mitochondria prepared from wild-type HEK293 cells was not significantly different from that imported into mitochondria from GRSF1 knockout HEK293 cells (Fig. 5E). Collectively, these data indicate that GRSF1 does not directly import *RMRP* into mitochondria but contributes to its accumulation in the matrix.

Impact of GRSF1 on the mitochondrial function of RMRP

While GRSF1 appeared important for retaining *RMRP* in the mitoplast, GRSF1 itself did not appear to transport *RMRP* through the mitochondrial membranes and into the matrix. The TOM/TIM machinery imports proteins from the cytosol through both mitochondrial membranes and into the matrix. PNPase is an RNA import factor

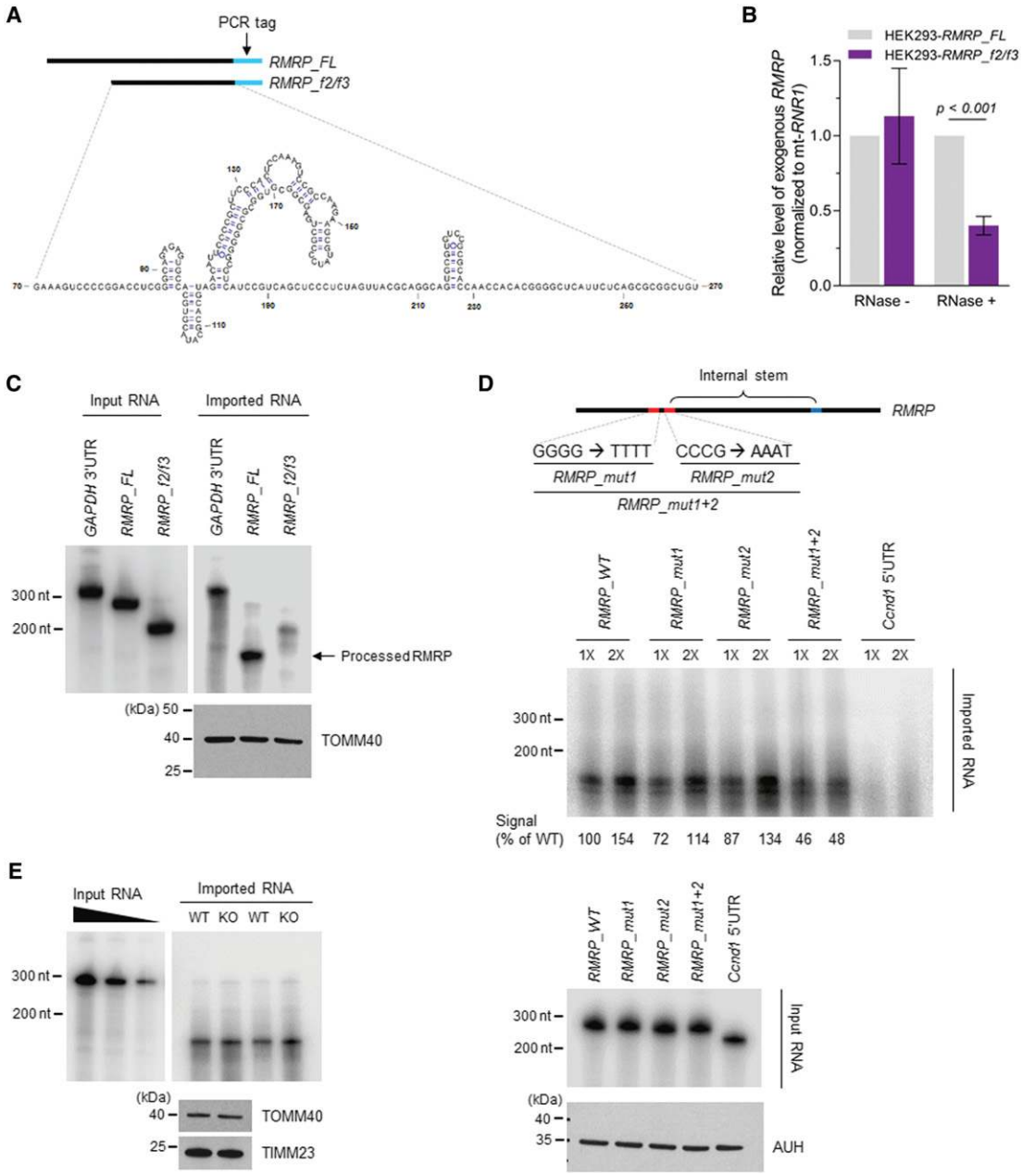

Figure 5. *RMRP* import assays. (*A*, *top*) Schematic depiction of *RMRP_FL* and *RMRP_f2/f3* harboring a PCR tag at the 3′ end that were cloned into plasmid pCDNA3. (*Bottom*) The predicted secondary structure of *RMRP_f2/f3*. (*B*) Mitoplasts isolated from clonal HEK293 populations expressing *RMRP_FL* or *RMRP_f2/f3* were treated with RNase A or left untreated, and the levels of each ectopic transcript were assayed by RT-qPCR analysis. (*C–E*) In vitro RNA import assays. (*C*) In vitro radiolabeled RNAs were incubated with mouse liver mitochondria for 15 min at 30°C. Nonimported RNA was eliminated with RNase A, and the remaining RNA was isolated and size-separated by electrophoresis through 6% urea polyacrylamide gels. TOMM40 Western blotting signals were included as loading control. (*D*) Radiolabeled wild-type or three mutant *RMRP*s ([mut1] G-rich; [mut2] stem sequence; [mut1+2] double mutant) were imported into mouse liver mitochondria. Import assays were performed as described in *B* using 1× and 2× amounts of radiolabeled RNAs. The mouse *Ccnd1* 5′ UTR was used as a negative control RNA, and AUH (detected by Western blot analysis) was the mitochondrial loading control. (*E*) Radiolabeled *RMRP* was imported into mitochondria isolated from wild-type or GRSF1 knockout HEK293 cells. TOMM40 and TIMM23 Western blot analyses served as loading controls. Data in *B* are the means and SD from three independent experiments. Data in *C–E* are representative of two experiments showing comparable results.

located in the IMS that mediates the translocation of cytosolic RNAs into mitochondria (Wang et al. 2010). Thus, we set out to investigate whether these transport factors were implicated in the import of *RMRP*. Silencing the TOM/TIM components TOMM40 and TIMM23 in wild-type and GRSF1 knockout HEK293 cells did not affect

PNPase levels, although it reduced the levels of the mitochondrial protein oxoglutarate dehydrogenase (OGDH) (Fig. 6A). Silencing PNPase did not affect the levels of other mitochondrial factors tested (Fig. 6B). Neither silencing intervention affected whole-cell *RMRP* levels (Fig. 6C, top), but each significantly lowered the levels of *RMRP* found in the mitoplast (Fig. 6C, bottom). These findings indicate that the PNPase and TOM/TIM machineries contribute to internalizing *RMRP*. In light of the fact that these effects were observed in both GRSF1-expressing and GRSF1-null cells, our findings indicate that the concentration of *RMRP* in the mitoplast is influenced by both the import via factors such as PNPase and TOM/TIM and the presence of GRSF1 in the mitoplast.

Next, we investigated whether the reduced *RMRP* abundance by GRSF1 depletion influenced mitochondrial functions. We first examined the impact of GRSF1 levels on cellular oxygen consumption rate (OCR) by using a Seahorse instrument. As shown in Figure 7A (left), silencing GRSF1 in HeLa cells impaired mitochondrial respiration, reduced basal OCR, and lowered ATP turnover rate (right); likewise, GRSF1 knockout clones (Fig. 4D) also displayed reduced OCR (Fig. 7B). We observed similar results from the basal OCR measurement by using the oxygen biosensor system (Supplemental Fig. S5A). Furthermore, a reduction of >25% in mtDNA copy number was also observed in GRSF1-depleted HEK293 cells (Supplemental Fig. S5B).

Interestingly, we found that ATP synthesis in whole-cell lysates was significantly inhibited by GRSF1 silencing (Fig. 7C, left), and this result might explain the increased phosphorylation of the AMP-activated protein kinase (AMPK) and reduced mitochondrial abundance of ATP5A, a subunit of mitochondrial ATP synthase (Fig. 7C, right). Although the level of cellular ATP is not a definitive measure of mitochondrial function (Brand and Nicholls 2011), our data support the idea that GRSF1 is important for maintaining mitochondrial OXPHOS capacity, glycolysis, and bioenergetic function as reported previously (Jourdain et al. 2013). We also sought to ask whether *RMRP* directly influenced mitochondrial metabolism. Using AS locked nucleic acids (LNAs) targeting *RMRP* in HeLa cells, *RMRP* levels declined to 45% of the levels seen in control HeLa cells (Fig. 7D, left). The reduction in *RMRP* led to a diminution of basal OCR level as measured using the Seahorse analysis (Fig. 7D, right); as anticipated, lowering *RMRP* levels also reduced the abundance of *mt-ATP6*, *mt-CO1*, and *mt-CYB* (Supplemental Fig. S5C).

Finally, we tested whether *RMRP* was implicated in the replication of mtDNA. Specifically, we tested whether the corresponding reduction in *RMRP* altered the primer-generating efficiency and, accordingly, the RNA–DNA transition sites. We performed ligation-mediated PCR (LMPCR) (Mueller and Wold 1989) to detect free 5′ ends of the newly synthesized mtDNA (H-strand origin) in both wild-type and GRSF1 knockout HEK293 cells using the strategy described previously (Kang et al. 1997) and detected the amplified DNA sequence by next-generation sequencing instead of conventional sequencing. As shown in Figure 7E, discrete positions were identified as major replication

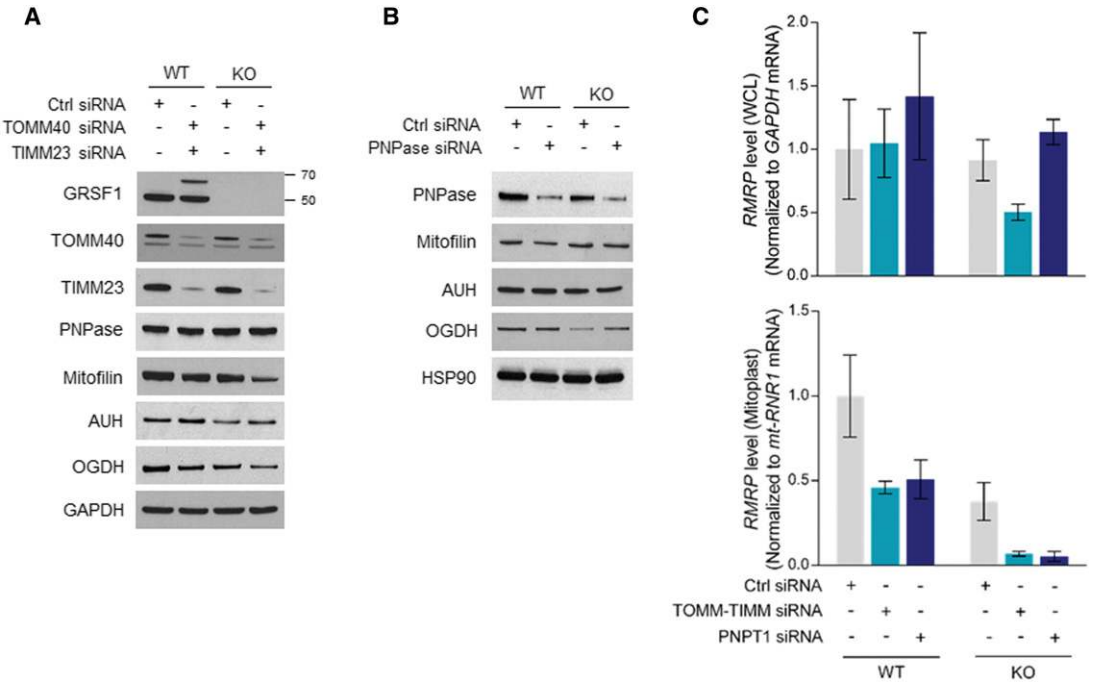

Figure 6. GRSF1 increases the mitochondrial retention of *RMRP*. (*A*,*B*) Forty-eight hours after silencing TOMM40 and TIMM23 (*A*) or PNPase (*B*) in wild-type and GRSF1 knockout HEK293 cells, Western blot analysis was used to detect the proteins shown. (*C*) RNA was prepared from whole cells or mitoplasts, and the levels of *RMRP* were determined by RT-qPCR analysis and normalized with *GAPDH* mRNA (*top*) or *mt-RNR1* (*bottom*).

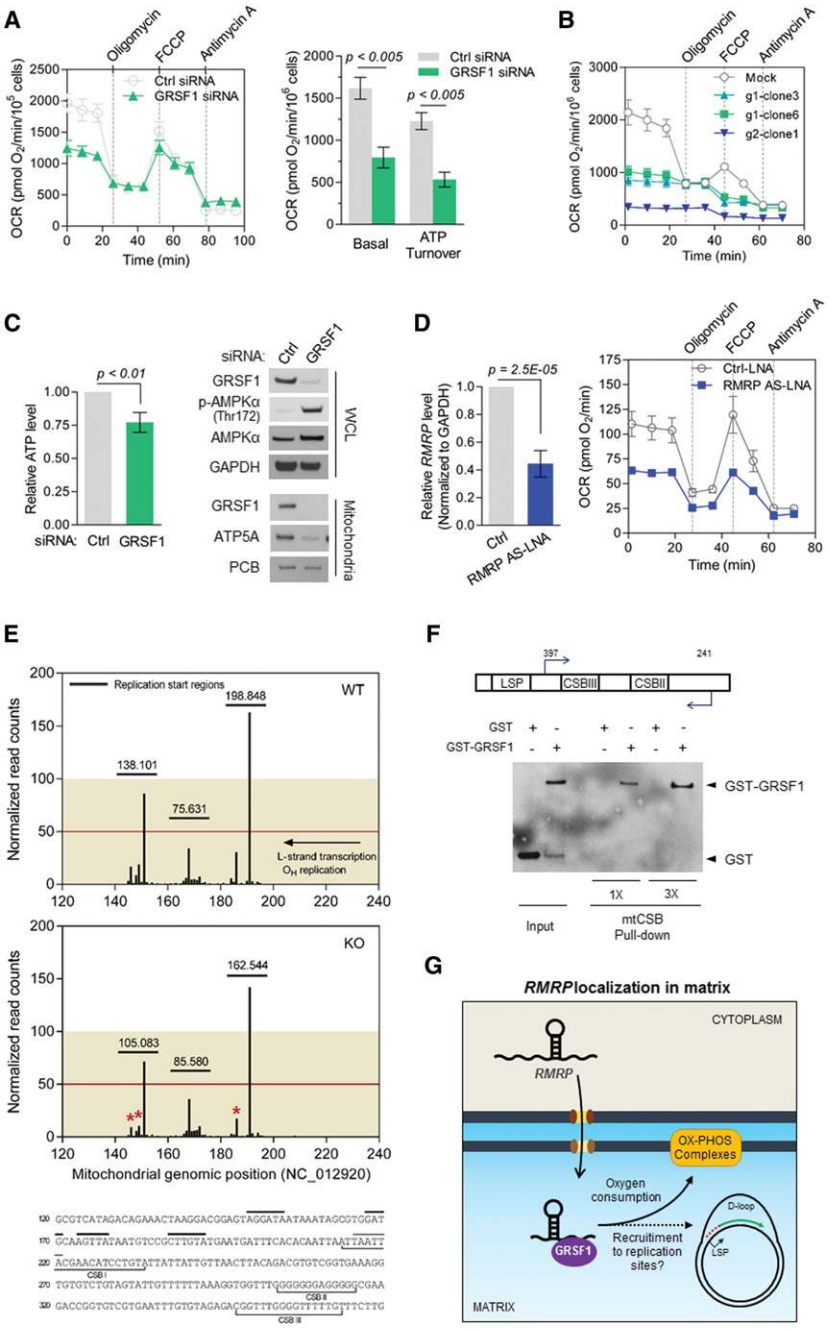

Figure 7. Depletion of GRSF1 impairs mitochondrial function. (*A*, *left*) Seahorse analysis to determine OCR in control and GRSF1 silenced HeLa cells under basal condition and after sequential injection of an ATPase inhibitor (oligomycin), a mitochondrial uncoupler (FCCP), and an electron transport inhibitor (antimycin A). $n = 4$. (*Right*) Basal OCR and ATP turnover were calculated. (*B*) OCR measurements were performed as in *A* in wild-type and GRSF1 knockout HEK293 clones described in Figure 4D. (*C*) Forty-eight hours after silencing GRSF1, whole-cell ATP levels were quantified, and Western blot analysis was performed to measure the levels of GRSF1, p-AMPKα (AMP-activated protein kinase [AMPK] phosphorylated at Thr172), and AMPKα in whole-cell lysates as well as GRSF1 and ATP5A in mitochondria. (*D*) Seventy-two hours after silencing *RMRP* using AS locked nucleic acid (LNA), the levels of remaining *RMRP* were quantified using RT-qPCR analysis (*left*), and OCR was measured as described in *A* (*right*). (*E*) Free 5′ ends of the newly synthesized mtDNA (O_H) from wild-type and GRSF1 knockout HEK293 cells were measured by isolating mtDNA, and the nascent mtDNA harboring free 5′ ends was amplified by ligation-mediated PCR (LMPCR). After ligating adapters to DNA fragments, paired-end RNA sequencing was performed. Normalized read counts were calculated at the single-nucleotide resolution and are shown as a bar graph (Supplemental Material). Asterisks indicate the positions at which GRSF1 knockout cells showed significantly lower read counts. (*F*, *top*) A mimic of the L-strand transcript harboring a G-rich sequence (spanning 82 nt upstream of and 75 nt downstream from the CSB II region) was transcribed in vitro in the presence of biotinylated CTP. (*Bottom*) The biotinylated RNA was then incubated with GST-tagged GRSF1 or control GST recombinant proteins. After pull-down using streptavidin beads, the presence of GRSF1 was detected by GST Western blot analysis. (*G*) Proposed function of GRSF1 enhancing mitochondrial retention of *RMRP* and *RMRP*-mediated primer generation for initiating mtDNA replication. The data in *A*–*D* represent the means and SD from three independent experiments. Data in *C* and *F* are representative of three different experiments.

initiation sites, similar to those found previously (Chang and Clayton 1985; Kang et al. 1997), although other sites (~nucleotide positions 220, 310, and 440) (described by Chang and Clayton 1985) were not detected, possibly due to the short segments of amplified DNA used for the library (<300 base pairs [bp]) (Supplemental Fig. S5D). As shown (Fig. 7E), the normalized read counts were significantly lower at several of the major 5′ end positions (at nucleotides 186, 149, and 146; $P = 0.0343$, 0.007, and 0.0004, respectively) in GRSF1 knockout cells relative to wild-type cells, suggesting that primer generation by *RMRP* enzyme activity was lower, and thus DNA replication efficiency was partly reduced in GRSF1 knockout cells.

Moreover, the light strand promoter (LSP) site contained several stretches of guanosine residues. Interestingly, the RNA sequence transcribed from the CSB II element (5′-GGGGGAGGGGGGG-3′) was proposed as a region of interaction with *RMRP* through its complementary sequence (5′-CGACCCCUCC-3′) (Chang and Clayton 1989). To test whether GRSF1 was also capable of binding the G-rich sequence in vitro, the biotinylated RNA corresponding to the L-strand transcript harboring the G-rich

sequence of CSB II was prepared (Fig. 7F, top) and incubated with GST-tagged GRSF1; pull-down analysis indicated that GRSF1 was capable of selectively binding this RNA sequence (Fig. 7F, bottom). Although the assay was performed in vitro, this result suggests that GRSF1 binds the imported *RMRP* and may guide the RNase MRP enzyme complex to the substrate RNA by targeting G-rich sequence within the CSB II transcript where *RMRP*-mediated cleavage occurs, and mtDNA replication can be initiated. Our results further suggest that the levels of *RMRP* in the mitoplast result from the combined impact of the TOM/TIM protein transport machinery, the RNA import activity of PNPase, and the association of *RMRP* with GRSF1 in the matrix. In summary, our results highlight a pathway by which *RMRP* transcribed from nuclear DNA is exported to the cytoplasm by HuR and is functionally enabled by GRSF1 in the matrix (Fig. 7G; Supplemental Fig. S6).

Discussion

mRNA RNP (mRNP) and lncRNA RNP (lncRNP) complexes

We identified two RBPs, HuR and GRSF1, responsible for mobilizing *RMRP* from the nucleus, where it is transcribed, to the mitochondria, where it functions as a constituent of the mitochondrial RNase MRP. The best-studied functions for RBPs are pre-mRNA splicing, mRNA turnover, and translation (Dreyfuss et al. 2002; Moore 2005; Keene 2007). Relatively less is known about the impact of RBPs on mRNA maturation, editing, transport, and storage, and still less is known about the impact of RBPs on the metabolism of lncRNAs, including lncRNA splicing, stability, and localization. The information emerging on lncRNA–RBP complexes (lncRNPs), systematically cataloged by Li et al. (2015), suggests that the same RBPs can bind coding RNA and ncRNA and affect their post-transcriptional fate in various ways. Indeed, there are increasing examples of RBPs that bind both mRNAs and lncRNAs; for example, HNRNPK binds *Oct1* mRNA and lncRNA *XIST* (Iwasaki et al. 2008; Chu et al. 2015), AUF1 binds *DICER1* mRNA and lncRNA *NEAT1* (Abdelmohsen et al. 2012; Yoon et al. 2014), and KSRP binds *NPM* mRNA and lncRNA *H19* (Cammas et al. 2014; Giovarelli et al. 2014).

Export of HuR RNPs

The main RBPs investigated here, HuR and GRSF1, have been found to bind both coding RNAs and ncRNAs. A vast collection of HuR target mRNAs have been identified and studied, including the *TP53*, *VHL*, *MYOD*, and *BCL2* mRNAs (Srikantan and Gorospe 2012). Several HuR target lncRNAs have also been described, including *lincRNA-p21* and *HOTAIR* (Yoon et al. 2012, 2013); many more have been identified by PAR-CLIP analysis (Lebedeva et al. 2011; Mukherjee et al. 2011). Collectively, for these target RNAs, HuR has been reported to primarily influence their relative stability and rates of translation. Less-understood functions of HuR include splicing, RNA storage in granules, and export of target RNAs.

HuR has been proposed to act as a key regulator of the nuclear export of several mRNAs (*CD83*, *COX2*/*PTGS2*, *FOS*, and *HuR*/*ELAVL1* mRNAs) (Gallouzi and Steitz 2001; Prechtel et al. 2006; Doller et al. 2008; Yi et al. 2010). Export of these mRNA ligands has been linked to the transport of HuR across the nuclear envelope, a process that requires the HuR nucleocytoplasmic shuttling domain (HNS) as well as several components of the transport machinery—primarily CRM1 but also transportins 1 and 2 and importin-1α. As shown in Figure 3, CRM1 was important for the export of nuclear HuR and *RMRP* to the cytosol. Phosphorylation of HuR by kinases Cdk1, PKC, and p38 also modulates its export to the cytoplasm (Eberhardt et al. 2012). It will be interesting to examine whether signaling pathways that trigger activation of these kinases modulate the nuclear export of HuR–*RMRP* complexes. Importantly, exposure to stress agents, which often require acute increases in ATP generation, can lower Cdk1 activity and increase PKC and p38 activities, all of which promote the export of HuR to the cytoplasm. It will be important to explore the possibility that specific stimuli may selectively regulate HuR–*RMRP* export to the cytoplasm. It will also be important to study whether HuR transports *RMRP* to the periphery of the mitochondria or instead releases *RMRP* upon exit to the cytoplasm, and other factors transport *RMRP* to the mitochondria.

HuR binding to target RNAs is also tightly regulated. Notably, kinases CHK2, p38, and PKC have been shown to alter HuR binding to specific mRNAs (Eberhardt et al. 2012). It will be interesting to determine whether these stress-activated kinases influence HuR binding to *RMRP* and whether binding is affected by stimuli that elicit mitochondrial responses.

GRSF1-facilitated localization of RMRP *in the mitochondrial matrix*

The other main RBP examined here, GRSF1, also interacts with mRNAs (e.g., the mitochondrial *GPX4* [m-*GPX4*] mRNA) (Ufer et al. 2008). Our results do not establish the precise pathways of *RMRP* transport through the OM, but *RMRP* is likely taken up via the generic import machinery (TOMM40 complex) to enter the IMS (Fig. 6). The transport of *RMRP* from the IMS to the matrix is not fully understood, but the ensuing presence of GRSF1–*RMRP* complexes in the matrix was associated with the accumulation of *RMRP* in the matrix (Fig. 4). A survey of GRSF1-binding partners in HEK293 cells (Jourdain et al. 2013) revealed an interaction between PNPase (PNPT1) and GRSF1; this was a provocative finding, as PNPase was localized in the IMS anchored to the IM and regulates the import of RNA into the matrix (for review, see Wang et al. 2010). We were unable to verify a physical interaction between PNPase and GRSF1 (data not shown) but did obtain evidence that the TOM/TIM import machinery was implicated in importing *RMRP* into the matrix (Fig. 6). We propose that, once *RMRP* reaches the matrix, GRSF1 associates with *RMRP* and increases

RMRP presence in the matrix (Fig. 4), in turn modulating *RMRP*'s impact on mitochondrial respiration and (albeit modestly) the generation of RNA primers for mtDNA replication (Fig. 7).

As shown in Figure 7, A and B, GRSF1 reduction or loss reduced mitochondrial respiration and lowered *RMRP* levels in the matrix (Fig. 4B,D). While suppressing *RMRP* levels also lowered mitochondrial respiration (Fig. 7D), the lower mitochondrial respiration due to loss of GRSF1 could not be definitively attributed to the reduced levels of *RMRP*, since GRSF1 binds to several mtDNA-encoded transcripts (*ND6* mRNA, lncRNAs *cytb*, and *ND5*) and regulates the abundance of numerous other mRNAs and encoded proteins (Antonicka et al. 2013).

Consequences of RMRP *mislocalization*

As the catalytic RNA component of RNase MRP, *RMRP* critically affects mitochondrial functions, including the initiation of mtDNA replication. Accordingly, *RMRP* mutations have been associated with certain pathologies, primarily the disease cartilage–hair hypoplasia (CHH), characterized by short stature, sparse hair, immune deficiencies, anemia, impaired bone growth, and increased cancer risk. The most frequent mutation (70A>G) (Hermanns et al. 2006) is in a region of putative interaction with GRSF1, adjacent to a G-rich stretch (Supplemental Fig. S5E), and perhaps interferes with the interaction of GRSF1 and *RMRP*. It will be interesting to test the relative affinity of wild-type *RMRP* and the 70A>G *RMRP* mutant. Another mutation described recently, 27G>C, disrupts base-pairing in the P3 domain of *RMRP* (Cherkaoui Jaouad et al. 2015). Interestingly, we found less abundance (Fig. 5B, in vivo support assay) and no maturation of *RMRP* in in vitro import assays after truncating the 5′ end of *RMRP*, including the P3 domain (Fig. 5C). These observations support the idea that CHH-causing mutations may affect sites of *RMRP* interaction with proteins important for *RMRP* function (e.g., RNase MRP) as well as *RMRP* transport and localization in mitochondria.

More globally, dysregulated mitochondrial function is associated with various different physiologic and pathologic processes in the cardiovascular, immune, neurological, and musculoskeletal systems. At present, GRSF1 has not been linked to specific diseases but was shown to be critical for controlling the differentiation of mammalian embryonic stem cells (Sampath et al. 2008). On the other hand, HuR has been linked extensively to the maintenance of organ homeostasis, for example, by modulating gastrointestinal function, cell senescence, cell proliferation, myogenesis, and the stress and immune responses (Srikantan and Gorospe 2012). HuR has also been implicated in numerous disease processes, including the prevention of neurodegenerative disease (Skliris et al. 2015) and the exacerbation of cancer, cardiovascular pathologies, and aberrant immune responses (Srikantan and Gorospe 2012; Suresh Babu et al. 2015).

A full understanding of how HuR-regulated mitochondrial function influences disease awaits further studies. However, recent reports have begun to link HuR to mitochondria-regulated processes; for example, in mice lacking HuR in B lymphocytes, aberrant mitochondrial function caused excess reactive oxygen species and B-cell death (Diaz-Muñoz et al. 2015). The neurodegeneration observed in mice lacking HuR in hippocampal neurons was also attributed to mitochondrial dysfunction due to an inability of the neurons to defend against oxidative damage or maintain energy homeostasis (Skliris et al. 2015). Similarly, in a mouse model of amyotrophic lateral sclerosis (ALS), mutant SOD sequestered HuR, thereby preventing its interaction with cellular mRNAs and triggering mitochondrial dysfunction, oxidative stress, and cell death (Lu et al. 2009). Investigating the contribution of *RMRP* nuclear export and mitochondria localization by HuR and GRSF1 will add critical insight into an expanding number of mitochondrial processes implicating coding and noncoding RNPs.

Materials and methods

Cell culture, transfection, and plasmids

Human HeLa and HEK293 cells were cultured in DMEM (Invitrogen) supplemented with 10% (v/v) FBS and antibiotics. All siRNAs, including control siRNA (UUCUCCGAACGUGUCACGUdTdT) and siRNAs targeting HuR (CGUAAGUUAUUUCCUUUAAdTdT), GRSF1 (GUGCCUCUCUGCUGCCGCA), IMMT (AAUUGCUGGAGCUGGCCUUUU), CRM1 (Santa Cruz Biotechnology, sc-35116), and PNPase (Santa Cruz Biotechnology, sc-61371), were transfected at 50 or 100 nM final concentration using Lipofectamine 2000 (Invitrogen) and analyzed 48 or 72 h later. Negative control or AS LNA oligomers targeting *RMRP* (Exiqon) were transfected at 30 nM final concentration. The plasmid expressing GRSF1 (pci-GRSF1-HA) and GRSF1-Flag-expressing HEK293 cells were previously reported (Jourdain et al. 2013). pMS2-YFP was described previously (Lee et al. 2010). Flag-tagged HuR was described previously (Yi et al. 2010). *RMRP_FL* and *RMRP_f2/f3* were cloned into pcDNA3 and used to generate stable cell lines expressing ectopic *RMRP*. CRISPR–Cas9 deletion of GRSF1 expression is explained in the Supplemental Material. TEM was performed using conventional methods (Supplemental Material).

Subcellular fractionation

Whole-cell, cytoplasmic, and nuclear fractions were prepared as explained in the Supplemental Material. Crude mitochondria and mitoplast and submitochondrial fractions were prepared as described in the Supplemental Material.

Protein analysis: Western blot, immunoprecipitation, and immunofluorescence

For Western blot analysis, protein lysates were prepared and analyzed as explained in the Supplemental Material. To detect mitochondrial interactions of GRSF1 with RNA, isolated mitochondria were lysed in mitochondrial extraction buffer, and immunoprecipitation was performed following the procedure as previously described (Jourdain et al. 2013) with minor modifications. Immunofluorescence analysis is explained in the Supplemental Material.

MS

Samples were separated by SDS-PAGE through a 4%–12% gradient gel and visualized by Coomassie brilliant blue staining. Protein bands were excised, and protein identification was performed at the Mass Spectrometry and Proteomics Facility, Johns Hopkins University. After in-gel trypsin digestion, trypsin-generated peptides were analyzed by liquid chromatography-coupled tandem MS (LC-MS/MS). Proteins were identified by matching tandem mass spectra with peptide sequences using the search software Mascot. After the database search, Scaffold software was used for validation of the identified peptides.

RNP analyses: RIP and biotin pull-down assay

RIP analysis from whole-cell extracts was carried out as previously described (Lee et al. 2010) and is explained in the Supplemental Material. To synthesize biotinylated transcripts, PCR fragments were prepared using forward primers that contained the T7 RNA polymerase promoter sequence, as described (Supplemental Material; Abdelmohsen et al. 2012). Primers used to prepare biotinylated transcripts are listed below (Supplemental Table S1).

RNA detection

Trizol (Invitrogen) was used to extract total RNA, and acidic phenol (Ambion) was used to extract RNA for RIP analysis (Lee et al. 2010). Reverse transcription was performed using random hexamers and reverse transcriptase (Invitrogen). qPCR was performed using gene-specific primers (Supplemental Table S1) and SYBR Green master mix (Kapa Biosystems) using the Applied Biosystems 7300 instrument.

RNA import assay

Measurement of RNA import assay into purified mitochondria was performed as previously described (Wang et al. 2010) with minor modifications. Detailed method for isolating purified mitochondria from mouse livers or HEK293 cells are described in the Supplemental Material.

Biotinylation and purification of 4-SU-labeled RNA

For metabolic labeling of nascent RNA, 4-SU (Sigma) was added to a 100 μM final concentration in the culture medium for 12 h. After RNA was extracted, 4SU-labeled RNA was biotinylated and pulled down using streptavidin beads, isolated, and used for RT-qPCR analysis (details are in the Supplemental Material).

Measurement of oxygen consumption

A Seahorse XF24 extracellular flux analyzer (Seahorse Biosciences) was used to measure OCR according to the manufacturer's instructions. Basal OCR was measured for 3 min every 8 min for four points, followed by sequential injection of 3 μM oligomycin, 1 μM FCCP, and 1 μM antimycin A. Each treatment was measured for 3 min every 8 min for three points. The number of live cells was counted (TC20, Bio-Rad) and used for data normalization.

Acknowledgments

We thank P. Ghosh, E. Lehrmann, and W.H. Wood III (National Institute on Aging, National Institutes of Health) for their assistance. This work was funded in its entirety by the National Institute on Aging-Intramural Research Program, National Institutes of Health.

References

Abdelmohsen K, Gorospe M. 2010. Posttranscriptional regulation of cancer traits by HuR. *Wiley Interdiscip Rev RNA* **1:** 214–229.

Abdelmohsen K, Tominaga-Yamanaka K, Srikantan S, Yoon JH, Kang MJ, Gorospe M. 2012. RNA-binding protein AUF1 represses Dicer expression. *Nucleic Acids Res* **40:** 11531–11544.

Anderson S, Bankier AT, Barrell BG, de Bruijn MH, Coulson AR, Drouin J, Eperon IC, Nierlich DP, Roe BA, Sanger F, et al. 1981. Sequence and organization of the human mitochondrial genome. *Nature* **290:** 457–465.

Antonicka H, Sasarman F, Nishimura T, Paupe V, Shoubridge EA. 2013. The mitochondrial RNA-binding protein GRSF1 localizes to RNA granules and is required for posttranscriptional mitochondrial gene expression. *Cell Metab.* **17:** 386–398.

Brand MD, Nicholls DG. 2011. Assessing mitochondrial dysfunction in cells. *Biochem J* **435:** 297–312.

Brennan CM, Gallouzi IE, Steitz JA. 2000. Protein ligands to HuR modulate its interaction with target mRNAs in vivo. *J Cell Biol* **151:** 1–14.

Cammas A, Sanchez BJ, Lian XJ, Dormoy-Raclet V, van der Giessen K, López de Silanes I, Ma J, Wilusz C, Richardson J, Gorospe M, et al. 2014. Destabilization of nucleophosmin mRNA by the HuR/KSRP complex is required for muscle fibre formation. *Nat Commun.* **5:** 4190.

Chang DD, Clayton DA. 1985. Priming of human mitochondrial DNA replication occurs at the light-strand promoter. *Proc Natl Acad Sci* **82:** 351–5.

Chang DD, Clayton DA. 1987. A mammalian mitochondrial RNA processing activity contains nucleus-encoded RNA. *Science* **235:** 1178–1184.

Chang DD, Clayton DA. 1989. Mouse RNAase MRP RNA is encoded by a nuclear gene and contains a decamer sequence complementary to a conserved region of mitochondrial RNA substrate. *Cell* **56:** 131–139.

Cherkaoui Jaouad I, Laarabi FZ, Chafai Elalaoui S, Lyonnet S, Henrion-Caude A, Sefiani A. 2015. Novel mutation and structural RNA analysis of the noncoding RNase MRP gene in cartilage-hair hypoplasia. *Mol Syndromol* **6:** 77–82.

Chu C, Zhang QC, da Rocha ST, Flynn RA, Bharadwaj M, Calabrese JM, Magnuson T, Heard E, Chang HY. 2015. Systematic discovery of xist RNA binding proteins. *Cell* **161:** 404–416.

Diaz-Muñoz MD, Bell SE, Fairfax K, Monzon-Casanova E, Cunningham AF, Gonzalez-Porta M, Andrews SR, Bunik VI, Zarnack K, Curk T, et al. 2015. The RNA-binding protein HuR is essential for the B cell antibody response. *Nat Immunol.* **16:** 415–425.

Doller A, Akool el-S, Huwiler A, Müller R, Radeke HH, Pfeilschifter J, Eberhardt W. 2008. Posttranslational modification of the AU-rich element binding protein HuR by protein kinase Cδ elicits angiotensin II-induced stabilization and nuclear export of cyclooxygenase 2 mRNA. *Mol Cell Biol* **28:** 2608–2625.

Dreyfuss G, Kim VN, Kataoka N. 2002. Messenger-RNA-binding proteins and the messages they carry. *Nat Rev Mol Cell Biol* **3:** 195–205.

Eberhardt W, Doller A, Pfeilschifter J. 2012. Regulation of the mRNA-binding protein HuR by posttranslational modification: spotlight on phosphorylation. *Curr Protein Pept Sci* **13:** 380–390.

Fan XC, Steitz JA. 1998. HNS, a nuclear-cytoplasmic shuttling sequence in HuR. *Proc Natl Acad Sci* **95:** 15293–15298.

Gallouzi IE, Steitz JA. 2001. Delineation of mRNA export pathways by the use of cell-permeable peptides. *Science* **294:** 1895–1901.

Gill T, Cai T, Aulds J, Wierzbicki S, Schmitt ME. 2004. RNase MRP cleaves the CLB2 mRNA to promote cell cycle progression: novel method of mRNA degradation. *Mol Cell Biol* **24:** 945–53.

Giovarelli M, Bucci G, Ramos A, Bordo D, Wilusz CJ, Chen CY, Puppo M, Briata P, Gherzi R. 2014. H19 long noncoding RNA controls the mRNA decay promoting function of KSRP. *Proc Natl Acad Sci* **111:** 5023–5028.

Hermanns P, Tran A, Munivez E, Carter S, Zabel B, Lee B, Leroy JG. 2006. RMRP mutations in cartilage–hair hypoplasia. *Am J Med Genet* **140A:** 2121–2130.

Iwasaki T, Koretomo Y, Fukuda T, Paronetto MP, Sette C, Fukami Y, Sato K. 2008. Expression, phosphorylation, and mRNA-binding of heterogeneous nuclear ribonucleoprotein K in *Xenopus* oocytes, eggs, and early embryos. *Dev Growth Differ* **50:** 23–40.

Jourdain AA, Koppen M, Wydro M, Rodley CD, Lightowlers RN, Chrzanowska-Lightowlers ZM, Martinou JC. 2013. GRSF1 regulates RNA processing in mitochondrial RNA granules. *Cell Metab* **17:** 399–410.

Kang D, Miyako K, Kai Y, Irie T, Takeshige K. 1997. In vivo determination of replication origins of human mitochondrial DNA by ligation-mediated polymerase chain reaction. *J Biol Chem* **272:** 15275–15279.

Keene JD. 2007. RNA regulons: coordination of post-transcriptional events. *Nat Rev Genet* **8:** 533–543.

Kishore S, Jaskiewicz L, Burger L, Hausser J, Khorshid M, Zavolan M. 2011. A quantitative analysis of CLIP methods for identifying binding sites of RNA-binding proteins. *Nat Methods* **8:** 559–564.

Lebedeva S, Jens M, Theil K, Schwanhausser B, Selbach M, Landthaler M, Rajewsky N. 2011. Transcriptome-wide analysis of regulatory interactions of the RNA-binding protein HuR. *Mol Cell* **43:** 340–352.

Lee EK, Kim HH, Kuwano Y, Abdelmohsen K, Srikantan S, Subaran SS, Gleichmann M, Mughal MR, Martindale JL, Yang X, et al. 2010. hnRNP C promotes APP translation by competing with FMRP for APP mRNA recruitment to P bodies. *Nat Struct Mol Biol* **17:** 732–739.

Li JH, Liu S, Zheng LL, Wu J, Sun WJ, Wang ZL, Zhou H, Qu LH, Yang JH. 2015. Discovery of protein–lncRNA interactions by integrating large-scale CLIP-seq and RNA-seq datasets. *Front Bioeng Biotechnol* **2:** 88.

Lu L, Wang S, Zheng L, Li X, Suswam EA, Zhang X, Wheeler CG, Nabors LB, Filippova N, King PH. 2009. Amyotrophic lateral sclerosis-linked mutant SOD1 sequesters Hu antigen R (HuR) and TIA-1-related protein (TIAR): implications for impaired post-transcriptional regulation of vascular endothelial growth factor. *J Biol Chem* **284:** 33989–33998.

Lygerou Z, Pluk H, van Venrooij WJ, Séraphin B. 1996. hPop1: an autoantigenic protein subunit shared by the human RNase P and RNase MRP ribonucleoproteins. *EMBO J* **15:** 5936–5948.

Maida Y, Yasukawa M, Furuuchi M, Lassmann T, Possemato R, Okamoto N, Kasim V, Hayashizaki Y, Hahn WC, Masutomi K. 2009. An RNA-dependent RNA polymerase formed by TERT and the RMRP RNA. *Nature* **461:** 230–235.

Mercer TR, Neph S, Dinger ME, Crawford J, Smith MA, Shearwood AM, Haugen E, Bracken CP, Rackham O, Stamatoyannopoulos JA, et al. 2011. The human mitochondrial transcriptome. *Cell* **146:** 645–658.

Moore MJ. 2005. From birth to death: the complex lives of eukaryotic mRNAs. *Science* **309:** 1514–1518.

Mueller PR, Wold B. 1989. In vivo footprinting of a muscle specific enhancer by ligation mediated PCR. *Science* **246:** 780–786.

Mukherjee N, Corcoran DL, Nusbaum JD, Reid DW, Georgiev S, Hafner M, Ascano M Jr, Tuschl T, Ohler U, Keene JD. 2011. Integrative regulatory mapping indicates that the RNA-binding protein HuR couples pre-mRNA processing and mRNA stability. *Mol Cell* **43:** 327–339.

Ohno M, Segref A, Bachi A, Wilm M, Mattaj IW. 2000. PHAX, a mediator of U snRNA nuclear export whose activity is regulated by phosphorylation. *Cell* **101:** 187–198.

Pluk H, van Eenennaam H, Rutjes SA, Pruijn GJ, van Venrooij WJ. 1999. RNA–protein interactions in the human RNase MRP ribonucleoprotein complex. *RNA* **5:** 512–524.

Prechtel AT, Chemnitz J, Schirmer S, Ehlers C, Langbein-Detsch I, Stülke J, Dabauvalle MC, Kehlenbach RH, Hauber J. 2006. Expression of CD83 is regulated by HuR via a novel *cis*-active coding region RNA element. *J Biol Chem* **281:** 10912–10925.

Qian Z, Wilusz J. 1994. GRSF-1: a poly(A)$^+$ mRNA binding protein which interacts with a conserved G-rich element. *Nucleic Acids Res* **22:** 2334–2343.

Sampath P, Pritchard DK, Pabon L, Reinecke H, Schwartz SM, Morris DR, Murry CE. 2008. A hierarchical network controls protein translation during murine embryonic stem cell self-renewal and differentiation. *Cell Stem Cell* **2:** 448–60.

Schmitt ME, Clayton DA. 1993. Nuclear RNase MRP is required for correct processing of pre-5.8S rRNA in *Saccharomyces cerevisiae*. *Mol Cell Biol* **13:** 7935–7941.

Skliris A, Papadaki O, Kafasla P, Karakasiliotis I, Hazapis O, Reczko M, Grammenoudi S, Bauer J, Kontoyiannis DL. 2015. Neuroprotection requires the functions of the RNA-binding protein HuR. *Cell Death Differ* **22:** 703–718.

Smirnov A, Comte C, Mager-Heckel AM, Addis V, Krasheninnikov IA, Martin RP, Entelis N, Tarassov I. 2010. Mitochondrial enzyme rhodanese is essential for *5S* ribosomal RNA import into human mitochondria. *J Biol Chem* **285:** 30792–30803.

Smirnov A, Entelis N, Martin RP, Tarassov I. 2011. Biological significance of 5S rRNA import into human mitochondria: role of ribosomal protein MRP-L18. *Genes Dev* **25:** 1289–1305.

Srikantan S, Gorospe M. 2012. HuR function in disease. *Front Biosci* **17:** 189–205.

Suresh Babu S, Joladarashi D, Jeyabal P, Thandavarayan RA, Krishnamurthy P. 2015. RNA-stabilizing proteins as molecular targets in cardiovascular pathologies. *Trends Cardiovasc Med* **25:** 676–683.

Ufer C. 2012. The biology of the RNA binding protein guanine-rich sequence binding factor 1. *Curr Protein Pept Sci.* **13:** 347–57.

Ufer C, Wang CC, Fähling M, Schiebel H, Thiele BJ, Billett EE, Kuhn H, Borchert A. 2008. Translational regulation of glutathione peroxidase 4 expression through guanine-rich sequence-binding factor 1 is essential for embryonic brain development. *Genes Dev* **22:** 1838–1850.

Wang G, Chen HW, Oktay Y, Zhang J, Allen EL, Smith GM, Fan KC, Hong JS, French SW, McCaffery JM, et al. 2010. PNPASE regulates RNA import into mitochondria. *Cell* **142:** 456–467.

Yi J, Chang N, Liu X, Guo G, Xue L, Tong T, Gorospe M, Wang W. 2010. Reduced nuclear export of HuR mRNA by HuR is linked

to the loss of HuR in replicative senescence. *Nucleic Acids Res* **38:** 1547–1558.

Yoon JH, Abdelmohsen K, Srikantan S, Yang X, Martindale JL, De S, Huarte M, Zhan M, Becker KG, Gorospe M. 2012. lincRNA–p21 suppresses target mRNA translation. *Mol Cell* **47:** 648–655.

Yoon JH, Abdelmohsen K, Kim J, Yang X, Martindale JL, Tominaga-Yamanaka K, White EJ, Orjalo AV, Rinn JL, Kreft SG, et al. 2013. Scaffold function of long non-coding RNA HOTAIR in protein ubiquitination. *Nat Commun* **4:** 2939.

Yoon JH, De S, Srikantan S, Abdelmohsen K, Grammatikakis I, Kim J, Kim KM, Noh JH, White EJ, Martindale JL, Yang X, et al. 2014. PAR-CLIP analysis uncovers AUF1 impact on target RNA fate and genome integrity. *Nat Commun* **5:** 5248.

HuR and GRSF1 modulate the nuclear export and mitochondrial localization of the lncRNA *RMRP*

Ji Heon Noh, Kyoung Mi Kim, Kotb Abdelmohsen, et al.

Genes Dev. 2016, **30:** originally published online May 19, 2016
Access the most recent version at doi:10.1101/gad.276022.115